

## Simulation of large-scale ice-sheet surges: The ISMIP HEINO experiments

Ralf Greve<sup>1\*</sup>, Ryoji Takahama<sup>2,1</sup> and Reinhard Calov<sup>3</sup>

<sup>1</sup>*Institute of Low Temperature Science, Hokkaido University, Kita-19, Nishi-8,  
Kita-ku, Sapporo 060-0819*

<sup>2</sup>*Graduate School of Environmental Science, Hokkaido University, Kita-10, Nishi-5,  
Kita-ku, Sapporo 060-0810*

<sup>3</sup>*Potsdam Institute for Climate Impact Research, PO Box 601203, D-14412 Potsdam, Germany*

*\*Corresponding author. E-mail: greve@lowtem.hokudai.ac.jp*

(Received February 28, 2006; Accepted August 25, 2006)

**Abstract:** The three-dimensional, dynamic/thermodynamic ice-sheet model SICOPOLIS (Simulation COde for POLythermal Ice Sheets) is applied to the ISMIP HEINO (Ice Sheet Model Intercomparison Project–Heinrich Event INtercOmparison) set-up. ISMIP HEINO has been designed to study large-scale ice-sheet instabilities, similar to those of the Laurentide ice sheet which are likely the cause of Heinrich events, on a simplified geometry which consists of a flat square with 4000 km side length. This square contains an area which resembles Hudson Bay and Hudson Strait, on which rapid sediment sliding can occur. The ice sheet is built up over 200 ka by assuming a temporally constant glacial climate. For the standard set-up of ISMIP HEINO, we obtain an oscillatory behaviour of the ice sheet with a main period of approx. 7.5 ka. One cycle consists of a gradual growth phase, followed by a massive surge through “Hudson Bay” and “Hudson Strait” owing to rapid sediment sliding on a molten bed. The occurrence of internal oscillations is robust against moderate variations of the surface boundary conditions and the strength of the sediment sliding. These findings support the idea of a free oscillatory mechanism as the main cause for large-scale ice-sheet surges.

**key words:** ice sheet, Heinrich event, instability, surge, model intercomparison

### 1. Introduction

Heinrich events (HEs), which have been discovered in North Atlantic sediments as layers of ice-rafted debris, are associated with quasi-periodic episodes of massive iceberg discharge from the Laurentide ice sheet through Hudson Bay and Hudson Strait into the Atlantic Ocean (Heinrich, 1988; Bond *et al.*, 1992; Broecker, 1994; Andrews, 1998; Clarke *et al.*, 1999). Six major events, labelled H1–H6, have been identified for the Wisconsinan Ice Age, with a recurrence interval between 7 ka and 13 ka. High resolution studies of deep sea cores have revealed that minor ice-rafting events occurred even more frequently at intervals of 2–3 ka (Bond and Lotti, 1995).

HEs are regarded as profound and catastrophic events, which are still poorly understood. Different glaciological mechanisms for ice-sheet instability, such as large-scale ice-stream surging, ice-shelf breakup and tidewater instability, or combinations of those, have

been considered. Based on a critical discussion of these possibilities and some computer modelling, Clarke *et al.* (1999) concluded that episodic surging of a large ice stream in Hudson Strait is the most plausible mechanism. A further problem is that HEs show a clear connection to climate change. They tend to occur at the culmination of a longer-term cooling cycle (Bond cycle) and are followed by a rapid warming; however, the cause-effect relationship between discharge events and climate changes is debated. From a glaciological point of view, climate-change-induced ice-sheet instability is difficult to explain, because the flow of an ice sheet is largely governed by its basal conditions, whereas climate forcings are imposed at the surface and propagate to the bed with substantial delay and attenuation (Clarke *et al.*, 1999). This favours the idea of an essentially intrinsic ice-sheet instability, which acts back on the climate system by the impact of massive iceberg discharge on the Atlantic thermohaline circulation.

MacAyeal (1993) proposed a “binge/purge” free oscillatory mechanism which explains HEs as transitions between two modes of operation of ice sheets, slow movement of ice over a frozen base *vs.* a fast sliding mode when the ice bed is molten. In subsequent studies by Payne (1995), Greve and MacAyeal (1996) and Hindmarsh and Le Meur (2001), multi-millennial internal oscillations of ice sheets were simulated with two-dimensional (one vertical and one horizontal direction) models. Marshall and Clarke (1997a,b) developed a three-dimensional model in order to investigate the role of ice streams in Hudson Strait in Heinrich-type events; however, they found only small-scale instabilities restricted to the area of the mouth of Hudson Strait. Calov *et al.* (2002) demonstrated for the first time that large-scale instabilities of the Laurentide ice sheet resembling HEs in periodicity, amplitude, spatial extent and discharge rate can be simulated with a three-dimensional dynamic/thermodynamic ice-sheet model (SICOPOLIS) coupled to an Earth system model (CLIMBER-2). Most recently, Papa *et al.* (2006) have used a simplified version of the model by Marshall and Clarke (1997a,b) with a parameterization of the basal sliding similar to Calov *et al.* (2002), and also succeeded in simulating millennial-scale oscillations of the Laurentide ice sheet under steady external forcing. These modelling progresses have further strengthened the plausibility of the internal-oscillation theory.

A challenge for the mechanism of a binge/purge-type internal oscillation is its apparent failure to explain almost synchronous discharges of icebergs from the North American and European ice sheets during HEs, because internal oscillations of different ice sheets should be independent of each other. However, Clarke *et al.* (1999) pointed out that conditions during climatic cooling episodes, such as at the culmination of a Bond cycle, are favourable for *triggering* large-scale ice-stream surging in Hudson Strait and elsewhere when the respective system is near the threshold of its intrinsic instability. Further, in the coupled ice-sheet-climate modelling study by Calov *et al.* (2002) it was explicitly demonstrated that a synchronization between instabilities of different ice sheets can be achieved by a *very weak* interaction or external forcing—a mechanism which resolves the apparent problem.

## 2. ISMIP HEINO

In order to investigate further the dependence of large-scale ice-sheet instabilities on atmospheric and basal conditions and compare the results of different ice-sheet models, the

ISMIP HEINO [Ice Sheet Model Intercomparison Project–Heinrich Event INtercOmparison; see Calov and Greve (2006) and <http://www.pik-potsdam.de/~calov/heino.html>] experiments have been devised. A simplified geometry resembling that of the EISMINT Phase 2 Simplified Geometry Experiments (Payne *et al.*, 2000) is employed. It consists of a flat, horizontal square with 4000 km side length, in which a circle of 2000 km radius defines the land area prone to glaciation. It is distinguished between hard rock and soft sediment, and the soft-sediment area has been chosen in order to resemble Hudson Bay and Hudson Strait (Fig. 1).

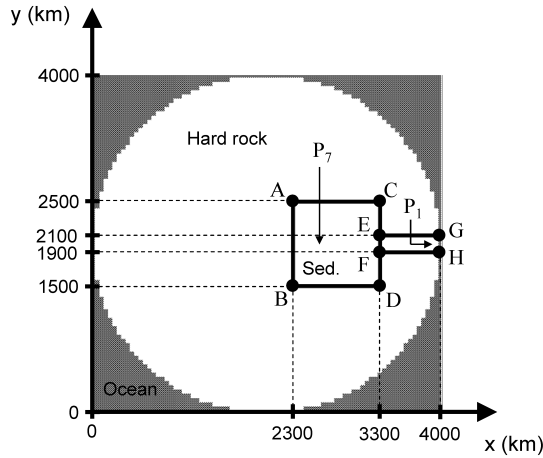


Fig. 1. Model domain of ISMIP HEINO (Calov and Greve, 2006). The land area is shown in white, the ocean is grey-shaded. The areas inside the square ABCD (“Hudson Bay”) and the rectangle EFGH (“Hudson Strait”) correspond to soft sediment. The remaining land area is hard rock. The positions of points  $P_1$  at the mouth of “Hudson Strait” and  $P_7$  inside “Hudson Bay” are indicated.

Since the objective of ISMIP HEINO is to study internal ice-sheet dynamics on a sub-Milankovitch time-scale, a steady (temporally constant) glacial climate is assumed. For the standard set-up (“ST”), the surface mass balance over the land area increases linearly from 0.15 m ice equiv.  $a^{-1}$  at the center to 0.3 m ice equiv.  $a^{-1}$  at the margin, and the surface temperature increases with the third power of distance from  $-40^\circ\text{C}$  at the center to  $-20^\circ\text{C}$  at the margin.

Rapid basal sliding is assumed for the sediment area (“Hudson Bay” and “Hudson Strait”) if the basal temperature reaches the pressure melting point. The sliding velocity  $v_b$  is then computed by using the linear sliding law

$$v_b = -\frac{C_s}{\rho g} \tau_b, \quad (1)$$

where  $C_s$  is the sediment-sliding parameter (standard value  $500 a^{-1}$ ).  $\tau_b = \rho g H S$  denotes the basal drag (shear stress), with the ice density  $\rho = 910 \text{ kg m}^{-3}$ , the acceleration due to gravity  $g = 9.81 \text{ m s}^{-2}$ , the ice thickness  $H$  and the ice-surface gradient (“slope”)  $S$ . By contrast, slow hard-bed sliding is assumed for the rock area, given by the Weertman-type sliding law

$$v_b = -\frac{C_R}{\rho g} \frac{\tau_b^3}{N_b^2}, \quad (2)$$

where  $C_R = 10^5 \text{ a}^{-1}$  is the rock-sliding parameter and  $N_b = \rho g H$  the basal normal stress. For both cases, no-slip conditions ( $v_b = 0$ ) are assumed when the basal temperature is below the pressure melting point. Note that, for simplicity, here the sliding laws are only given in scalar form and for the shallow-ice approximation (see below, Section 3). For the general case see Calov and Greve (2006).

The sediment-sliding law (1) can be justified by assuming shear deformation of a linear-viscous sediment layer of viscosity  $\mu$  and constant thickness  $d$ , which yields  $C_S = \rho g d / \mu$ . In view of the conceptual approach pursued by ISMIP HEINO, this is a reasonable simplification of the slightly non-linear viscoplastic behaviour found by Jenson (1994) for sediment samples taken in northern Illinois, about 70 km inside the terminus of the late-Wisconsinan Lake Michigan Lobe of the Laurentide ice sheet. By adopting a shear-layer thickness of  $d = 2$  m, which is an average value of Jenson's (1994) calculated thicknesses, the lower boundary of his measured range of sediment viscosities ( $\mu = 5.2 \times 10^9 \text{ Pa s}$ ) corresponds to a value of  $C_S$  of approximately  $100 \text{ a}^{-1}$ . Since active lubrication caused by basal melting of an overlying ice mass further reduces the sediment viscosity, this value is considered as the minimum of plausible values, and for the parameter studies of ISMIP HEINO (see below, Section 4.3)  $C_S$  is varied between  $100 \text{ a}^{-1}$  and  $1000 \text{ a}^{-1}$ , with a standard value of  $500 \text{ a}^{-1}$  as noted above. The hard-rock-sliding law (2) and the value of  $C_R$  are those of Greve *et al.* (1998).

Note that, even though the numerical value of  $C_S$  is smaller than that of  $C_R$ , the sediment sliding is much stronger than the hard-rock sliding. This is so, because the additional factor  $\tau_b^2 / N_b^2 (= S^2)$  in eq. (2) is of the order of  $10^{-6}$ , so that the sliding velocities resulting from eq. (1) are typically three orders of magnitude larger than those resulting from eq. (2). For example, a local ice thickness of 3 km and a surface slope of  $0.2^\circ$  yields a sediment-sliding velocity of  $\approx 5 \text{ km a}^{-1}$  and a rock-sliding velocity of  $\approx 10 \text{ m a}^{-1}$  (Takahama, 2006).

The set of physical parameters applied for the standard set-up of ISMIP HEINO is listed in Table 1.

Table 1. Physical parameters of the standard ISMIP HEINO set-up (Calov and Greve, 2006).

Quantity	Value
Gravity acceleration, $g$	$9.81 \text{ m s}^{-2}$
Density of ice, $\rho$	$910 \text{ kg m}^{-3}$
Power-law exponent, $n$	3
Flow-enhancement factor, $E$	3
Melting point at atmospheric pressure, $T_0$	273.15 K
Heat conductivity of ice, $\kappa$	$2.1 \text{ W m}^{-1} \text{ K}^{-1}$
Specific heat of ice, $c$	$2009 \text{ J kg}^{-1} \text{ K}^{-1}$
Latent heat of ice, $L$	$335 \text{ kJ kg}^{-1}$
Clausius-Clapeyron gradient, $\beta$	$8.7 \times 10^{-4} \text{ K m}^{-1}$
Sliding parameter for hard rock, $C_R$	$10^5 \text{ a}^{-1}$
Sliding parameter for soft sediment, $C_S$	$500 \text{ a}^{-1}$
Geothermal heat flux, $q_{\text{geo}}$	$42 \text{ mW m}^{-2}$

### 3. Ice-sheet model SICOPOLIS

For this study, we use the ice-sheet model SICOPOLIS (“SIMulation COde for POLythermal Ice Sheets”), which simulates the large-scale dynamics and thermodynamics (ice extent, thickness, velocity, temperature, water content and age) of ice sheets three-dimensionally and as a function of time (Greve, 1997). It is based on the shallow-ice approximation (*e.g.*, Hutter, 1983) and the rheology of an incompressible, heat-conducting power-law fluid [Glen’s flow law, see Paterson (1994)]. Boundary conditions (surface temperature, surface mass balance, basal sliding, geothermal heat flux) are prescribed according to the HEINO set-up (see Section 2).

Finite differences on a quadratic grid, aligned along the  $x$ - and  $y$ -axes (see Fig. 1), are employed in order to solve the model equations. For all simulations, the horizontal resolution is 50 km, which leads to  $81 \times 81$  grid points in the model domain. The model time is from  $t=0$  until  $t=200$  ka, starting from ice-free initial conditions, and the time-step is 0.25 a, which follows the recommendation by Calov and Greve (2006) (see also below, Section 4.5).

## 4. Results and discussion

### 4.1. Standard run

In the standard run ST, defined by the above set-up, the ice sheet is built up during the first 25 ka. After that, the volume of the simulated ice sheet oscillates with a main period of approx. 7500 years and an amplitude (understood as *full* difference between maximum and minimum) of about  $2 \times 10^6$  km<sup>3</sup> around an average value of  $\approx 36 \times 10^6$  km<sup>3</sup> (Fig. 2). By assuming an oceanic area of  $3.62 \times 10^8$  km<sup>2</sup>, these figures correspond to an average volume of 90 m sea-level equivalent and an oscillation amplitude of 5 m sea-level equivalent on the real Earth.

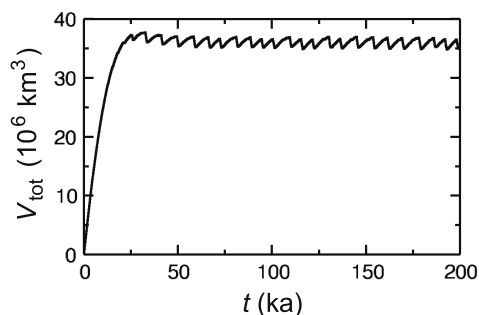


Fig. 2. Total ice volume,  $V_{\text{tot}}$ , as function of time for run ST.

In the following, we will focus on the last 50 ka of the model time ( $t=150\dots 200$  ka) and on the sediment area (“Hudson Bay” and “Hudson Strait”) defined in Fig. 1. The temporal evolution of the average ice thickness over the sediment area (Fig. 3, top panel) is highly correlated to the total ice volume discussed in the previous paragraph. The main 7500-year period is evident, and the amplitude of the oscillations is about 1 km. One full

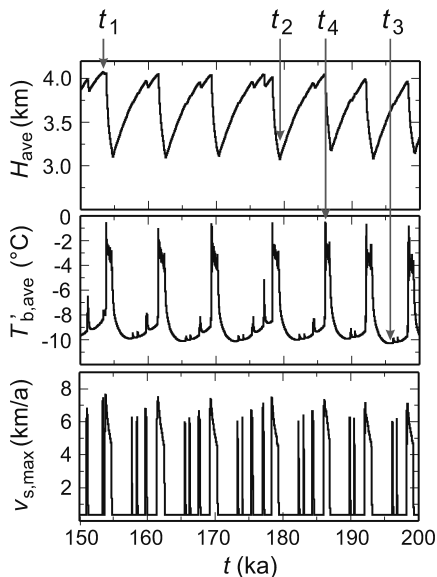


Fig. 3. Time series of run ST (for the last 50 ka only): average ice thickness,  $H_{\text{ave}}$ , average basal temperature relative to pressure melting,  $T'_{\text{b,ave}}$ , and maximum surface velocity,  $v_{\text{s,max}}$ . Quantities refer to the sediment area shown in Fig. 1. For times  $t_1$ – $t_4$  see main text.

cycle consists of a gradual growth phase ( $\approx 6500$  years), followed by a massive surge ( $\approx 1000$  years). During the growth phase, basal temperatures are below pressure melting for most of the sediment area (Fig. 3, middle panel), and the ice flows slowly by internal deformation only (Fig. 3, bottom panel). Owing to increasing thermal insulation against the cold surface, basal temperatures rise gradually, until the pressure melting point is reached at the mouth of “Hudson Strait”. At that time, rapid basal sliding sets in, which leads to increased strain heating. As a consequence, a thermal wave (“activation wave”) develops, which travels upstream very quickly until almost the entire sediment area is at pressure melting. The surge starts, develops flow velocities of up to  $8 \text{ km a}^{-1}$ , and the ice sheet suffers a strong collapse, which goes on until the reduced thermal insulation and the enhanced downward advection of cold surface ice causes the basal temperatures to fall below pressure melting again. Then the surge comes to a halt, and the next growth phase begins.

In addition to the main oscillations, the signal of the maximum surface velocity (Fig. 3, bottom panel) shows a number of additional, higher-frequency peaks, which are only slightly reflected in the signals of the ice thickness and the basal temperature. In this case, rapid sediment sliding remains limited to the mouth of “Hudson Strait”, because the increased strain heating is not strong enough to initiate a fully developed activation wave. This behaviour, which was already reported by Calov *et al.* (2002), is illustrated very nicely in Fig. 4. The local ice thickness at the point  $P_7$  in the interior of “Hudson Bay” reflects essentially the main 7500-year cycle, whereas the thickness at  $P_1$  close to the mouth of “Hudson Strait” shows oscillations at a much higher frequency. Also, the power spectrum of the average ice thickness (Fig. 5) shows clearly that the main oscillation, which manifests itself as a double peak centered around approx. 7500 years, is accompanied by some minor peaks at periods between 1000 and 5500 years. It is striking that this finding agrees very well with high-resolution deep-sea records which show that the main HEs were accompanied by more frequent minor discharge events, as mentioned in Section 1.

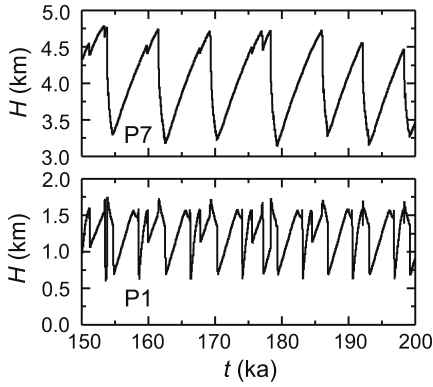


Fig. 4. Time series of run ST (for the last 50 ka only): local ice thickness at points  $P_7$  (top panel) and  $P_1$  (bottom panel), respectively. For the positions of  $P_1$  and  $P_7$  see Fig. 1.

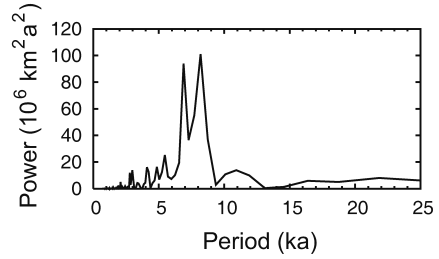


Fig. 5. Power spectrum of the average ice thickness  $H_{\text{ave}}$  of run ST (see Fig. 3, top panel).

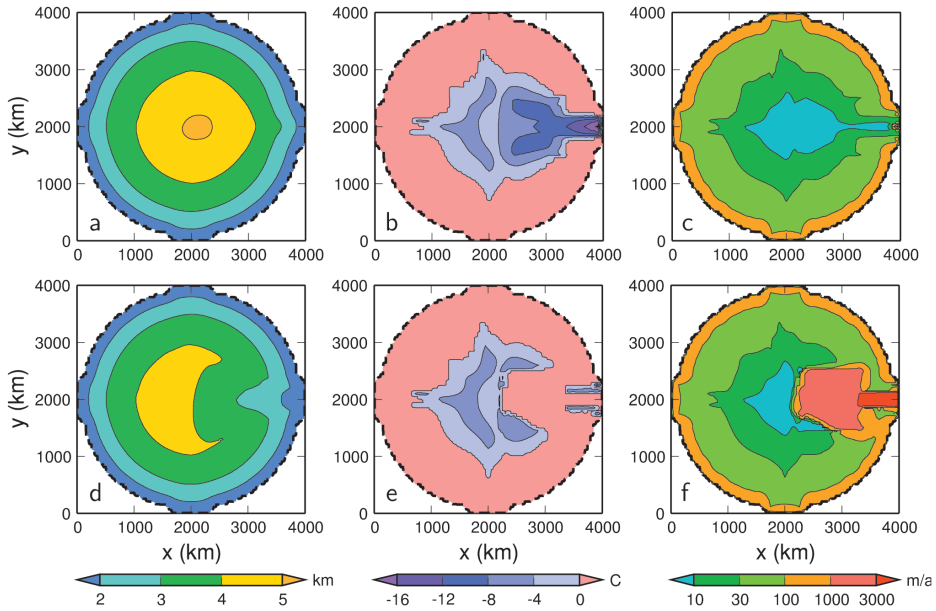


Fig. 6. Phases of a Heinrich event (HE). (a) Ice thickness at time  $t_1$ , (b) basal temperature relative to pressure melting at time  $t_1$ , (c) surface velocity at time  $t_1$  (before a HE). (d) Ice thickness at time  $t_2$  (after a HE). (e) Basal temperature relative to pressure melting at time  $t_2$ , (f) surface velocity at time  $t_2$  (during a HE).

According to the ISMIP HEINO description (Calov and Greve, 2006), the times  $t_1$ – $t_4$  are defined as the times of maximum ( $t_1$ ) and minimum ( $t_2$ ) average ice thickness, minimum average basal temperature ( $t_3$ ) and maximum basal area at pressure melting ( $t_4$ ) for the sediment region during the period from  $t = 150$  to  $200$  ka. These times are indicated in Fig. 3,

and snapshots of the state of the ice sheet at  $t_1$  (before surge),  $t_2$  (after surge) and  $t_4$  (during surge) are shown in Fig. 6. Comparison of panels (a) and (d) shows very impressively the different topographies of the ice sheet before and after a surge. While before a surge the surface is essentially radially symmetric with respect to the center, after the surge the part over the sediment region has lowered by about 1 km and leaves a huge surface depression. The different distributions of the basal temperature and surface velocity before and during a surge are illustrated by the pairs of panels (b), (e) and (c), (f), respectively. Before a surge, basal temperatures are low and flow velocities are small ( $< 100 \text{ m a}^{-1}$ ) for the entire sediment area. This contrasts strongly with the high basal temperatures and flow velocities ( $> 1000 \text{ m a}^{-1}$ ) during the surge.

Evidently, the fields shown in Fig. 6 are not fully symmetric with respect to the line  $y = 2000 \text{ km}$ , whereas the geometry and boundary conditions are. Since the SICOPOLIS code has been carefully checked for asymmetries of that kind and did not show such symmetry-breaking in the EISMINT Phase 2 Simplified Geometry Experiments (Payne *et al.*, 2000), we speculate that the asymmetry results from the compilation or execution of the Fortran code in conjunction with the great sensitivity of the detailed instability process to small changes in the local conditions.

#### 4.2. Variations of the surface boundary conditions

In order to investigate the robustness and sensitivity of the simulated large-scale surges, in the ISMIP HEINO description (Calov and Greve, 2006) a series of runs with varied surface boundary conditions are specified. These are in detail:

- Run T1: surface temperature decreased by  $10^\circ\text{C}$ .
- Run T2: surface temperature increased by  $10^\circ\text{C}$ .
- Run B1: surface accumulation reduced by a factor 2.
- Run B2: surface accumulation increased by a factor 2.

Figure 7 shows the results of these simulations for the average ice thickness over the sediment region. While for run ST, it oscillates between approx. 3.1 and 4.1 km, the interval is from 3.5 to 4.5 km for the colder run T1 and from 2.5 to 3.2 km for the warmer run T2. This is so because the lower the surface temperatures are, the thicker the ice sheet must grow before thermal insulation can melt the ice base and initiate an activation wave. Also, the shape of the oscillations is affected, in that the ratio of the durations of the surge phase and the growth phase becomes larger with increasing surface temperature. By contrast, the period of the oscillations does not change significantly for runs ST, T1 and T2.

This is different for the runs B1 and B2 with varied accumulation rate. Naturally, smaller surface accumulation entails smaller ice thickness (variation between 2.5 and 3.5 km for run B1) and larger surface accumulation entails larger ice thickness (variation between 3.5 and 4.5 km for run B2), but in addition a distinct impact on the period of the oscillations becomes evident. The main period is about 14500 years for run B1 and about 4500 years for run B2. This is due to the fact that the accumulation rate affects directly the growth time required to build up the ice sheet to the critical thickness at which a surge can be released. Also, the larger the accumulation rate, the larger the average ice thickness and the more fiercely the surge proceeds, so that the duration of the surge phase is also shorter.

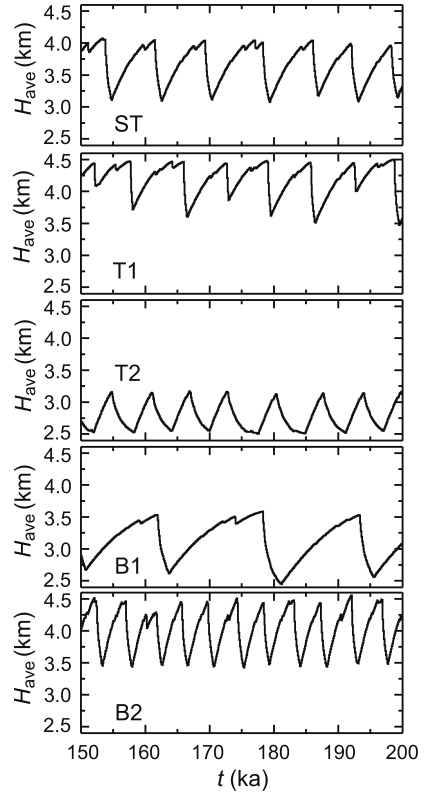


Fig. 7. Time series of the average ice thickness over the sediment area,  $H_{\text{ave}}$ , for runs ST, T1, T2, B1 and B2 (standard run, surface temperature  $10^{\circ}\text{C}$  lower/higher, surface accumulation reduced/increased by a factor 2, respectively).

#### 4.3. Variations of the basal sliding

In addition to the variations of the surface boundary conditions discussed above, the ISMIP HEINO description (Calov and Greve, 2006) defines simulations with changed sediment-sliding parameter  $C_S$ :

- Run S1:  $C_S = 100 \text{ a}^{-1}$ .
- Run S2:  $C_S = 200 \text{ a}^{-1}$ .
- Run S3:  $C_S = 1000 \text{ a}^{-1}$ .

Results for the average ice thickness over the sediment region are shown in Fig. 8. For all values of  $C_S$ , significant oscillations occur. However, sediment sliding is the crucial process for the occurrence of large-scale surges, and it is therefore not surprising that a significant influence of the parameter  $C_S$  becomes evident. The amplitude of the oscillations increases monotonically from approximately 0.5 km (S1) via 0.6 km (S2) and 1.0 km (ST) to 1.4 km (S3). Also, the shape of the oscillations is altered strongly, in that the surge phases change from rather gradual surface lowerings to very abrupt collapses. The period of the oscillations is affected to a much lesser extent; only in run S1 (weakest sediment sliding) the prolonged surge phases cause the period to increase distinctly.

In the ISMIP HEINO sliding laws for soft sediment and hard rock, eqs. (1) and (2), respectively, it is assumed that basal sliding occurs only if the ice base is at pressure melting ( $T_b' = 0^{\circ}\text{C}$ ) and that no-slip conditions prevail otherwise ( $T_b' < 0^{\circ}\text{C}$ ). Hindmarsh and Le Meur (2001) proposed to replace this binary switch by a continuous formulation which

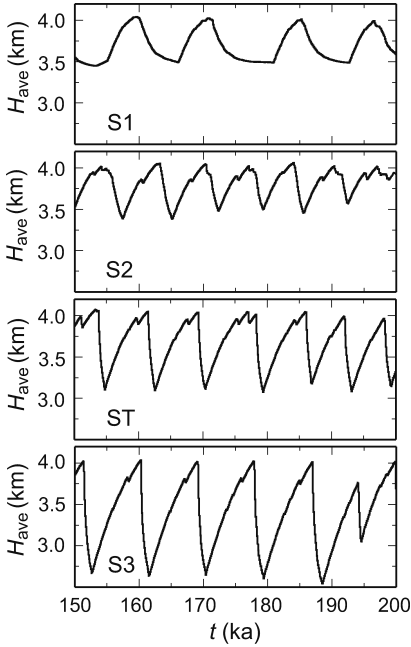


Fig. 8. Time series of the average ice thickness over the sediment area,  $H_{ave}$ , for runs S1, S2, ST and S3 (sediment-sliding parameter  $C_s=100, 200, 500$  and  $1000 a^{-1}$ , respectively).

allows for sub-melt sliding,

$$v_b(T_b') = v_b(T_b' = 0^\circ\text{C}) \times e^{T_b'/\gamma}, \quad (3)$$

where  $T_b'$  is the basal temperature relative to pressure melting (note that  $T_b' \leq 0^\circ\text{C}$ ),  $v_b(T_b' = 0^\circ\text{C})$  is the fully developed sliding according to eqs. (1) and (2), respectively, and  $\gamma$  is the sub-melt-sliding parameter. This sliding law was introduced mainly because of its greater numerical stability, but it can be physically supported by arguing that melting occurs in sub-grid patches at the ice base when the grid-cell averaged basal temperature approaches the melting point. It was used in a recent study by Greve (2005) for parameterizing the hard-rock sliding of the Greenland ice sheet. However, a problem is that there is no theoretical or experimental basis for the value of the parameter  $\gamma$ .

We test the effect of sub-melt sliding on the dynamics of the ISMIP HEINO ice sheet by re-running the standard simulation with the following settings:

- Run G02:  $\gamma = 0.2^\circ\text{C}$ .
- Run G05:  $\gamma = 0.5^\circ\text{C}$ .
- Run G1:  $\gamma = 1^\circ\text{C}$ .

Note that it is assumed that the same value of  $\gamma$  holds for sediment sliding and hard-rock sliding. The value for run G1 ( $\gamma = 1^\circ\text{C}$ ) was employed by Hindmarsh and Le Meur (2001) and Greve (2005), but this choice was made for reasons of numerical stability only.

Figure 9 shows the results. It is evident that the influence of sub-melt sliding on the ice-sheet oscillations is pronounced. For run G02, the oscillation amplitude has increased to  $\approx 1.3$  km, and the period length has increased to  $\approx 11000$  years, mainly due to the prolonged surge phases. It is also striking that the oscillations are highly regular in comparison to those of run ST. In the cases of runs G05 and G1, the ice thickness is reduced strongly and

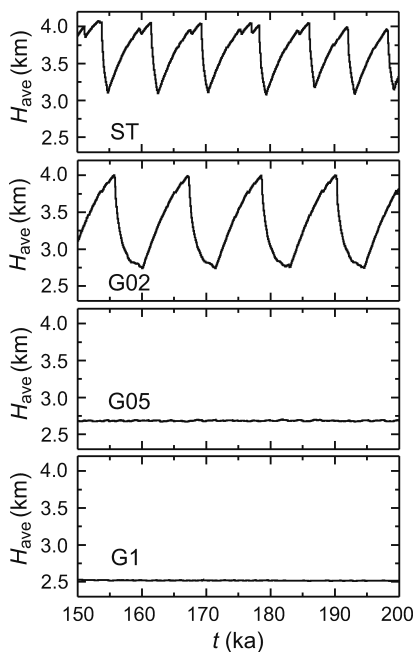


Fig. 9. Time series of the average ice thickness over the sediment area,  $H_{ave}$ , for runs ST, G02, G05 and G1 (sub-melt-sliding parameter  $\gamma=0, 0.2, 0.5$  and  $1^\circ\text{C}$ , respectively).

the oscillations have essentially disappeared. The ice sheet remains permanently in an intermediate surging state, in which the surging area extends over “Hudson Strait” and parts of “Hudson Bay”, and the maximum surface velocity is always larger than  $2.83 \text{ km a}^{-1}$  (for G05) and  $3.06 \text{ km a}^{-1}$  (for G1), respectively.

As mentioned above, sub-melt sliding can be physically interpreted as the effect of sub-grid-scale patchiness of the basal conditions. For the recent West Antarctic ice sheet, it is known that small-scale variations of basal conditions on soft beds exist as “sticky spots” of the ice streams entering the Ross ice shelf (*e.g.*, MacAyeal, 1992). If similar conditions prevailed for the Laurentide ice sheet, a non-zero value of the sub-melt-sliding parameter  $\gamma$  cannot be ruled out. On the other hand, the results of runs G05 and G1 are clearly unrealistic, because, as mentioned above, they predict a continuously active ice stream over “Hudson Strait”. Such a scenario would become manifest in a continuous record of ice-rafted debris in North Atlantic sediments, which is in clear contradiction to the observed debris layers between normal marine sediments. Therefore, we think that sub-melt sliding is only of little relevance for the large-scale, rapid sediment sliding in Hudson Bay and Hudson Strait, and that the real situation is best approximated by a vanishing or a very small value of the sub-melt-sliding parameter  $\gamma$ .

#### 4.4. Rotated sediment mask

For the EISMINT Phase 2 Simplified Geometry Experiments (SGE) on a circular ice sheet with radially symmetric forcing, it was observed that under certain circumstances the symmetry is broken by the formation of radial spokes of cold ice which extend from the interior of the ice sheet outward into the surrounding zone of basal melt (Payne *et al.*, 2000). It is not clear whether these spokes, which also manifest themselves in the surface

topography and velocity distributions, are related to a real-world phenomenon (thermomechanical instability, fingering), or whether they are numerical artifacts provoked by the quadratic grid of the SGE set-up (see also Saito *et al.*, 2006).

The situation is not directly comparable with the ISMIP HEINO set-up. Nevertheless, it will now be investigated to what extent the simulated large-scale ice-sheet surges are influenced by the alignment of the numerical grid to the square/rectangular sediment area (Fig. 1). To this end, Takahama (2006) has re-run the standard run ST nine times, where the sediment area has been rotated by  $5^\circ$ ,  $10^\circ$ , ...,  $45^\circ$  around the center  $(\hat{x}, \hat{y}) = (2000 \text{ km}, 2000 \text{ km})$  of the quadratic model domain. Since the HEINO set-up is radially symmetric with respect to the center, theoretically these rotations should not alter the simulation results, and any changes are due to effects of the quadratic grid which breaks this symmetry.

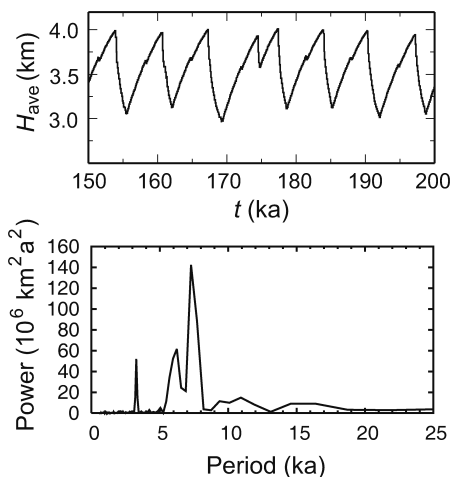


Fig. 10. Run ST\_ROT45 (sediment mask rotated by  $45^\circ$ ): average ice thickness over the sediment area (top panel), power spectrum of the average ice thickness (bottom panel).

Here, we only report the result of run ST\_ROT45 with a rotation angle of  $45^\circ$ . In this case, the sediment area points toward the top right corner of the model domain (Fig. 1). Figure 10 shows the average ice thickness over the sediment area and the associated power spectrum. Comparison with the respective results of run ST (Fig. 3, top panel, and Fig. 5) demonstrates that, while some fine structures of the temporal evolution and the power spectrum are influenced by the rotation, the maximum and minimum ice thickness and the main period of the oscillations are essentially unaffected. The same behaviour was noted by Takahama (2006) for other rotation angles. This is a strong support for the statement that the internal oscillations are a robust feature (at least in the SICOPOLIS model) and not merely a numerical artifact caused by some favourable alignment of the numerical grid.

#### 4.5. Time-step and grid resolution

Takahama (2006) presents sensitivity tests on the time-step for the set-up of the stan-

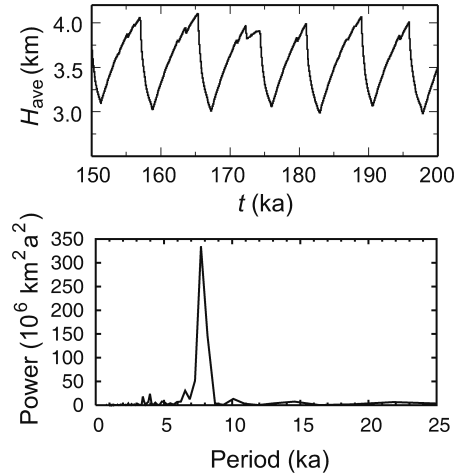


Fig. 11. Run ST\_DX25 (doubled horizontal resolution): average ice thickness over the sediment area (top panel), power spectrum of the average ice thickness (bottom panel).

dard run ST. Up to and including a time-step of 2 a, the simulations are numerically stable. However, as the time-step is reduced to 1 a, 0.5 a and finally 0.25 a, the main period of the oscillations decreases from approx. 9300 to 7500 years, and also the amplitude decreases slightly. For 0.25 a, reasonable convergence is achieved, even though the fine structure of the oscillations still shows some differences compared to 0.5 a. Therefore, we consider a time-step of 0.25 a an acceptable compromise between convergence and computing time.

In order to investigate the influence of grid resolution, the standard run ST with 50 km resolution has been re-run with a doubled resolution of 25 km (run ST\_DX25). The time-step (0.25 a) has been kept. The main effect of the higher resolution is that the average volume of the oscillating ice sheet is  $\approx 37 \times 10^6 \text{ km}^3$ , approximately 3% larger than that of run ST. Also, the fine structure and the exact timing of the oscillations are somewhat influenced, whereas their amplitude, period and ratio of surge to growth phases remain essentially unchanged (Fig. 11). This finding demonstrates once again the robustness of the simulated oscillations.

## 5. Conclusion

The ice-sheet model SICOPOLIS operated at the Institute of Low Temperature Science, Hokkaido University, has successfully provided large-scale ice-sheet surges for the ISMIP HEINO set-up. The occurrence of these surges is robust against moderate variations of the surface temperature, surface accumulation and sediment sliding. Additional experiments have shown that strong sub-melt sliding has the potential to level out the ice-sheet oscillations; however, this is likely not representative for the real situation of sediment sliding. Rotations of the sediment mask with respect to the numerical grid and changes of the grid resolution leave the oscillations essentially unaffected. These findings support the idea that Heinrich events are essentially the result of internal ice-sheet dynamics

and thermodynamics and do not depend crucially on external climate variability. Since Calov *et al.* (2002) demonstrated the possibility of a synchronisation of ice-sheet surges by a *very weak* interaction or external forcing, this does not contradict the apparent occurrence of almost synchronous discharge events of icebergs from the North American and European ice sheets.

Within the frame of the ongoing Ice Sheet Model Intercomparison Project (ISMIP), the ISMIP HEINO experiments will be carried out by other working groups with different ice-sheet models. It will be instructive to learn whether the occurrence, amplitude and periodicity of such internal oscillations are robust features or not across the variety of existing ice-sheet models, and which model improvements can be done to better capture the striking phenomenon of ice-sheet instability.

### Acknowledgments

This study is based on the master thesis by Takahama (2006). The authors wish to thank T. Hondoh and S. Sugiyama for co-supervising the thesis, and P. Huybrechts for coordinating the Ice Sheet Model Intercomparison Project (ISMIP). The paper has significantly benefited from the reviews by F. Saito and two anonymous referees.

### References

- Andrews, J.T. (1998): Abrupt changes (Heinrich events) in late Quaternary North Atlantic marine environments: a history and review of data and concepts. *J. Quaternary Sci.*, **13**, 3–16.
- Bond, G., Heinrich, H., Huon, S., Broecker, W., Labeyrie, L., Andrews, J., McManus, J., Clasen, S., Tedesco, K., Jantschik, R., Simet, C. and Klas, M. (1992): Evidence for massive discharges of icebergs into the glacial Northern Atlantic. *Nature*, **360** (6401), 245–250.
- Bond, G.C. and Lotti, R. (1995): Iceberg discharges into the North Atlantic on millennial time scales during the last glaciation. *Science*, **267** (5200), 1005–1010.
- Broecker, W.S. (1994): Massive iceberg discharges as triggers for global climate change. *Nature*, **372** (6505), 421–424.
- Calov, R. and Greve, R. (2006): ISMIP HEINO. Ice Sheet Model Intercomparison Project–Heinrich Event IntercOmparison. Available online at <http://www.pik-potsdam.de/~calov/heino.html>.
- Calov, R., Ganopolski, A., Petoukhov, V., Claussen, M. and Greve, R. (2002): Large-scale instabilities of the Laurentide ice sheet simulated in a fully coupled climate-system model. *Geophys. Res. Lett.*, **29** (24), 2216. doi: 10.1029/2002GL016078.
- Clarke, G.K.C., Marshall, S.J., Hillaire-Marcel, C., Bilodeau, G. and Veiga-Pires, C. (1999): A glaciological perspective on Heinrich events. *Mechanisms of Global Climate Change at Millennial Time Scales*, ed. by P.U. Clark *et al.* Washington, D.C., Am. Geophys. Union, 243–262 (Geophysical Monograph No. 112).
- Greve, R. (1997): Application of a polythermal three-dimensional ice sheet model to the Greenland ice sheet: Response to steady-state and transient climate scenarios. *J. Climate*, **10**, 901–918.
- Greve, R. (2005): Relation of measured basal temperatures and the spatial distribution of the geothermal heat flux for the Greenland ice sheet. *Ann. Glaciol.*, **42**, 424–432.
- Greve, R. and MacAyeal, D.R. (1996): Dynamic/thermodynamic simulations of Laurentide ice-sheet instability. *Ann. Glaciol.*, **23**, 328–335.
- Greve, R., Weis, M. and Hutter, K. (1998): Palaeoclimatic evolution and present conditions of the Greenland ice sheet in the vicinity of Summit: An approach by large-scale modelling. *Paleoclimates*, **2** (2–3), 133–161.
- Heinrich, H. (1988): Origin and consequences of cyclic ice rafting in the Northeast Atlantic Ocean during the past 130,000 years. *Quaternary Res.*, **29**, 142–152.
- Hindmarsh, R.C.A. and Le Meur, E. (2001): Dynamical processes involved in the retreat of marine ice sheets. *J. Glaciol.*, **47**, 271–282.

- Hutter, K. (1983): *Theoretical Glaciology; Material Science of Ice and the Mechanics of Glaciers and Ice Sheets*. Dordrecht, D. Reidel, 548 p.
- Jenson, J.W. (1994): A nonlinear numerical model of the Lake Michigan lobe, Laurentide ice sheet. Doctoral thesis, Department of Geology, Oregon State University, Corvallis, Oregon, U.S.A.
- MacAyeal, D.R. (1992): The basal stress distribution of ice stream E, Antarctica, inferred by control methods. *J. Geophys. Res.*, **97** (B1), 595–603.
- MacAyeal, D.R. (1993): Binge/purge oscillations of the Laurentide ice sheet as a cause of the North Atlantic's Heinrich events. *Paleoceanography*, **8**, 775–784.
- Marshall, S.J. and Clarke, G.K.C. (1997a): A continuum mixture model of ice stream thermomechanics in the Laurentide Ice Sheet 1. Theory. *J. Geophys. Res.*, **102** (B9), 20599–20613.
- Marshall, S.J. and Clarke, G.K.C. (1997b): A continuum mixture model of ice stream thermomechanics in the Laurentide Ice Sheet 2. Application to the Hudson Strait ice stream. *J. Geophys. Res.*, **102** (B9), 20615–20637.
- Papa, B.D., Mysak, L.A. and Wang, Z. (2006): Intermittent ice sheet discharge events in northeastern North America during the last glacial period. *Climate Dyn.*, **26** (2–3), 201–216, doi: 10.1007/s00382-005-0078-4.
- Paterson, W.S.B. (1994): *The Physics of Glaciers*. Oxford, Pergamon Press, 3rd ed.
- Payne, A.J. (1995): Limit cycles in the basal thermal regime of ice sheets. *J. Geophys. Res.*, **100** (B3), 4249–4263.
- Payne, A.J., Huybrechts, P., Abe-Ouchi, A., Calov, R., Fastook, J.L., Greve, R., Marshall, S.J., Marsiat, I., Ritz, C., Tarasov, L. and Thomassen, M.P.A. (2000): Results from the EISMINT model intercomparison: the effects of thermomechanical coupling. *J. Glaciol.*, **46**, 227–238.
- Saito, F., Abe-Ouchi, A. and Blatter, H. (2006): European ice sheet modelling initiative (EISMINT) model intercomparison experiments with first-order mechanics. *J. Geophys. Res.*, **111** (F2), F02012, doi: 10.1029/2004JF000273.
- Takahama, R. (2006): Heinrich Event Intercomparison with the ice-sheet model SICOPOLIS. Master thesis, Graduate School of Environmental Science, Hokkaido University, Sapporo, Japan.